# INDEX

**Acronyms**

| | |
|---|---|
| CFD | computational fluid dynamics |
| RTD | residence time distribution |
| LES | large eddy simulation |
| DNS | direct numerical simulation |
| RANS | Reynolds averaged Navier-Stokes equations |
| RSM | Reynolds stress model |
| CoV | coefficient of variation |
| LDA | laser Doppler anemometry |
| LDV | laser Doppler velocimetry |
| PIV | particle image velocimetry |

**Examples are identified in bold face type**

*Cross references are italicized*




*Handbook of Industrial Mixing: Science and Practice*, Edited by Edward L. Paul, Victor A. Atiemo-Obeng, and Suzanne M. Kresta
ISBN 0-471-26919-0 

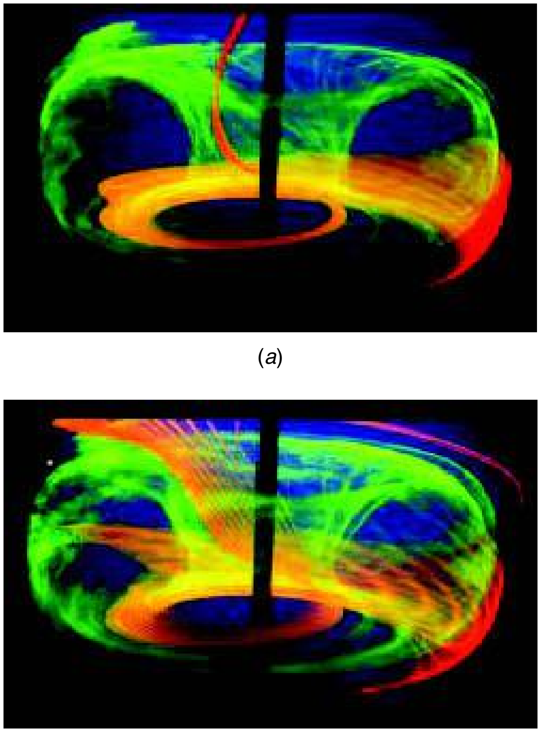

(*a*)

(*b*)

**Figure 3-8** The complex mixing patterns formed by chaotic flows are highly heterogeneous, and understanding the emerging structure is crucial to predicting heat and mass transfer in these systems. Here, some experimental pictures are shown of the mixing pattern formed by colored fluorescent dye in a stirred tank. The time evolution of the emerging structure can be monitored if a series of snapshots are taken in time, as in (*a*) and (*b*).

*Handbook of Industrial Mixing: Science and Practice*, Edited by Edward L. Paul,
Victor A. Atiemo-Obeng, and Suzanne M. Kresta
ISBN 0-471-26919-0 

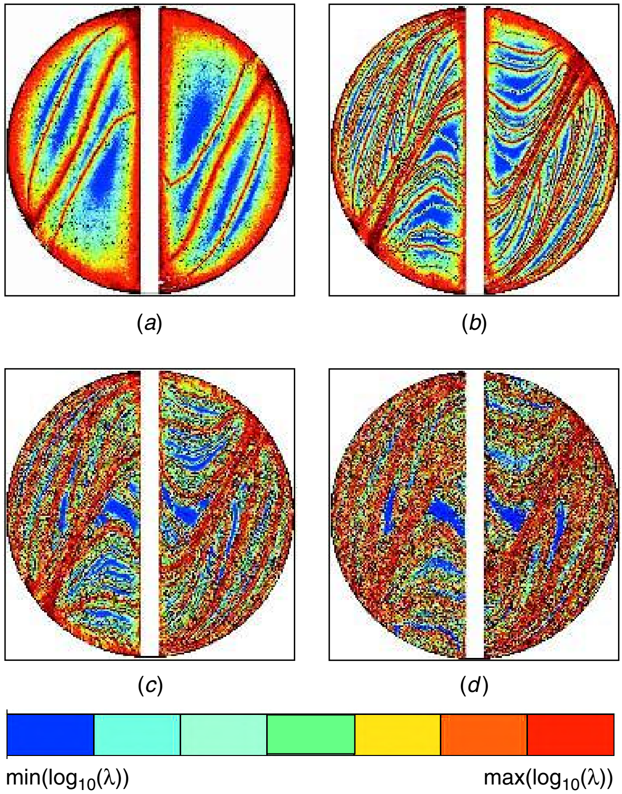


**Figure 3-21** Contours of the stretching field in the standard Kenics mixer at $\mathrm{Re} = 10(10)^{1/3}$. The cross-sectional planes correspond to axial distances after $(a)$ 2, $(b)$ 6, $(c)$ 10, and $(d)$ 22 mixer elements.

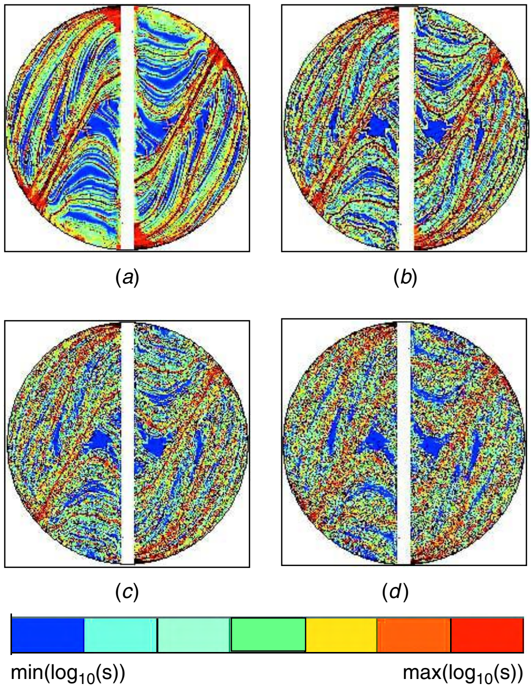


**Figure 3-23** Intermaterial area density (ρ) from coarse-grained stretching average in the standard Kenics mixer at $\mathrm{Re} = 10(10)^{1/3}$ after (*a*) 8, (*b*) 12, (*c*) 16, and (*d*) 22 mixer elements.

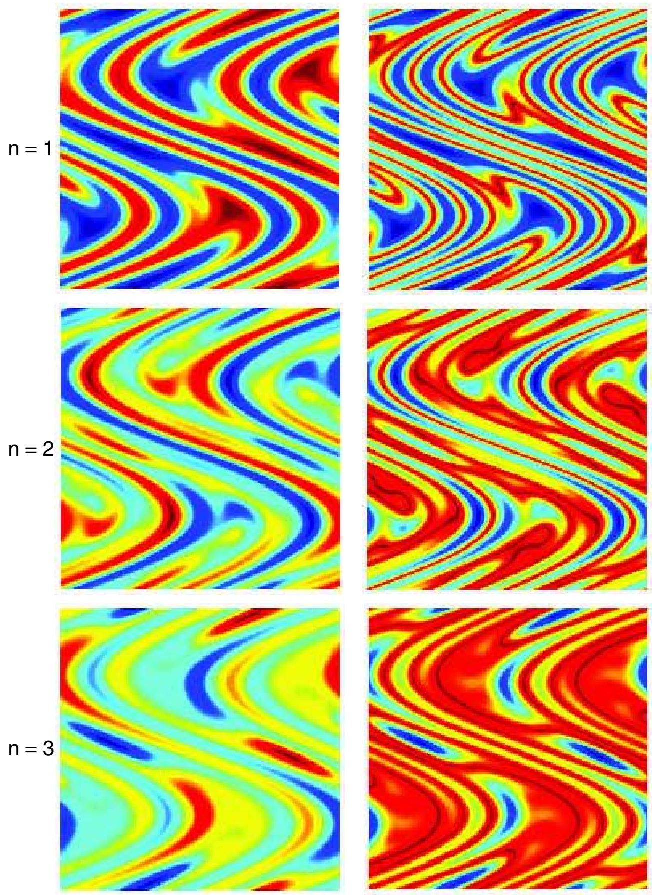


**Figure 3-28** The left-hand side of the figure shows the concentration of reactants A and B after the first three flow periods in the sine flow with $T = 1.6$. The right-hand side is the corresponding product concentration.

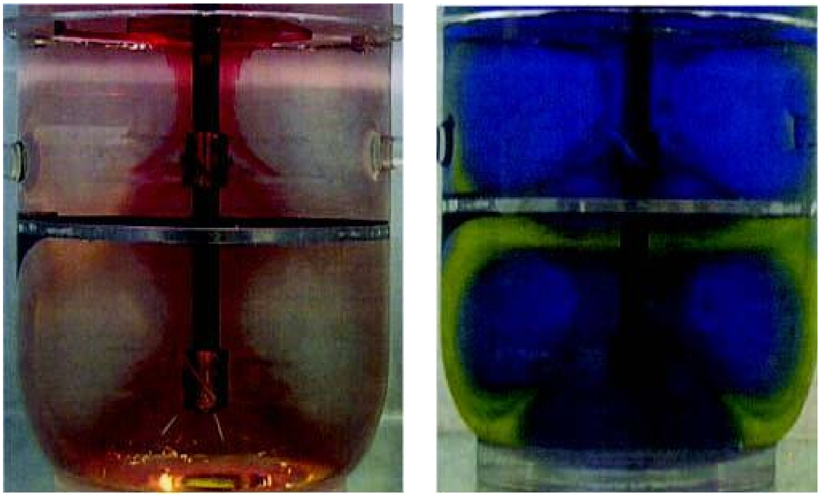

(*a*) (*b*)

**Figure 4-13** Red dye tracer addition (*a*) and acid–base decolorization using bromophenol blue (*b*). (From Clark and Özcan-Taşkin, 2001.)

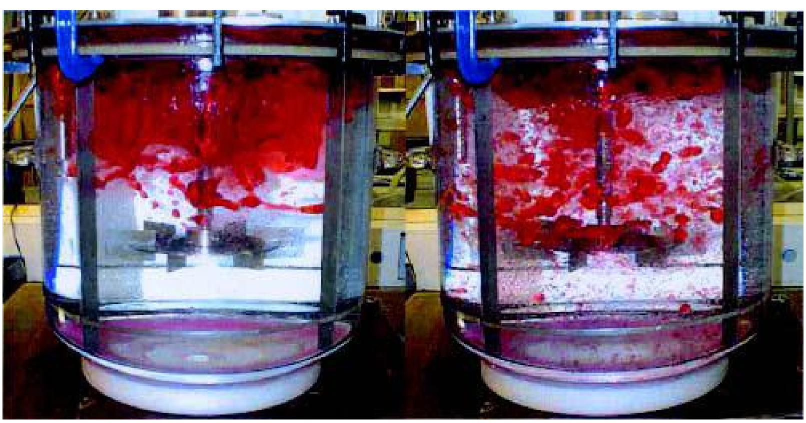

**Figure 4-24** Immiscible liquid–liquid system at a speed below that required for complete dispersion.

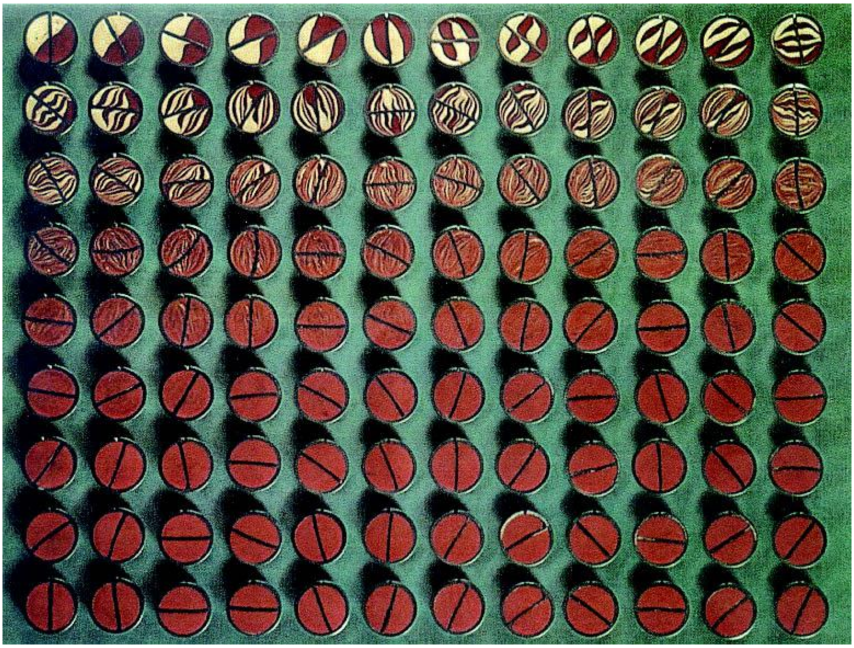

**Figure 7-20** Laminar mixing of fluids by division and recombination (KMS mixer). Cross-sections of the mixer are shown in sequence from left to right, top to bottom. (Courtesy of Chemineer, Inc.)

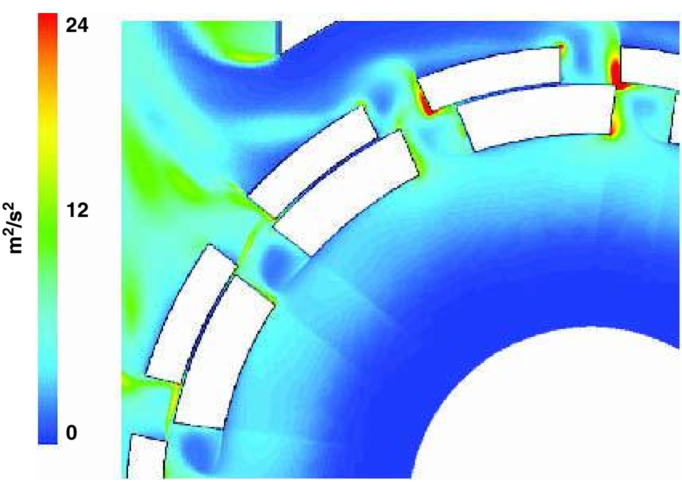


**Figure 8-12** Turbulent kinetic energy ($m^2/s^2$) from 2D CFD simulation for IKA prototype mixer. Single-time snapshot.

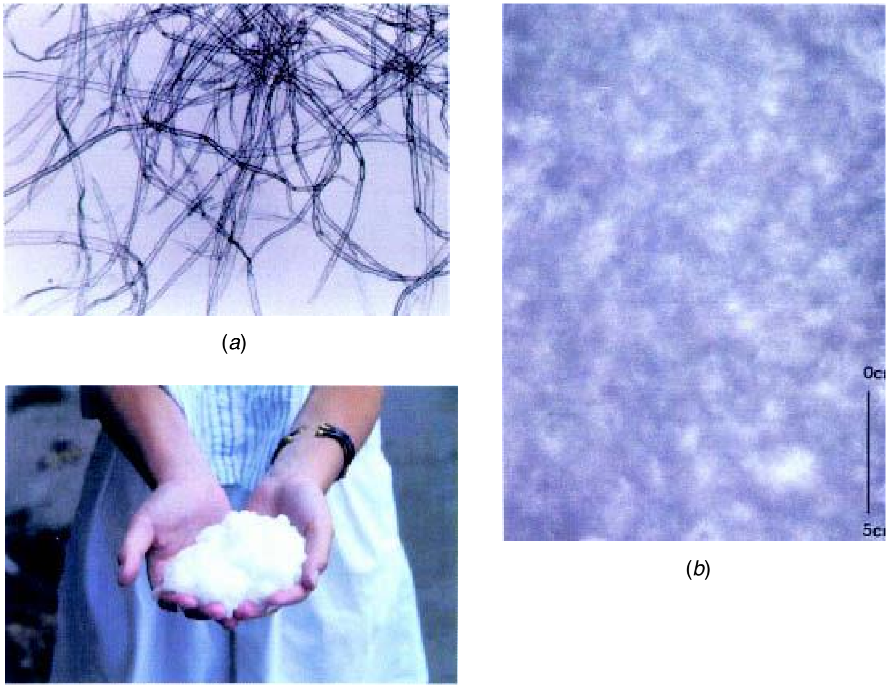


**Figure 20-4** Photographs of fibers and suspensions: (*a*) photomicrograph of softwood trachieds ($l_w = 2.37$ mm); (*b*) light transmission through a $C_m = 0.005$ kraft pulp suspension showing mass nonuniformities (flocs). The line in the image is 5 cm in length; (*c*) hands hold a medium consistency ($C_m = 0.10$) kraft pulp suspension.

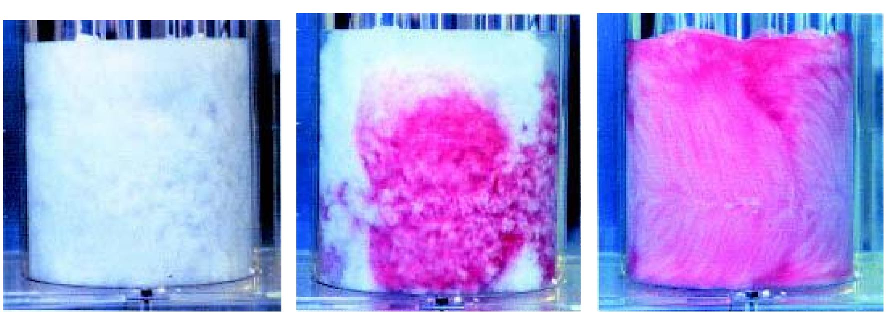

(a) (b) (c)

**Figure 20-6** Effect of yield stress on suspension motion in a stirred tank. $C_m = 0.02$ FBK suspension. The vessel is 30 cm in diameter with the suspension height set at 30 cm. A $D = 10$ cm diameter Rushton turbine was located 10 cm from the vessel floor. Impeller speeds are $N =$ (*a*) 4, (*b*) 7, and (*c*) 14 rps. The red dye shows regions of suspension motion. In image (*a*) the cavern has not reached the vessel wall.

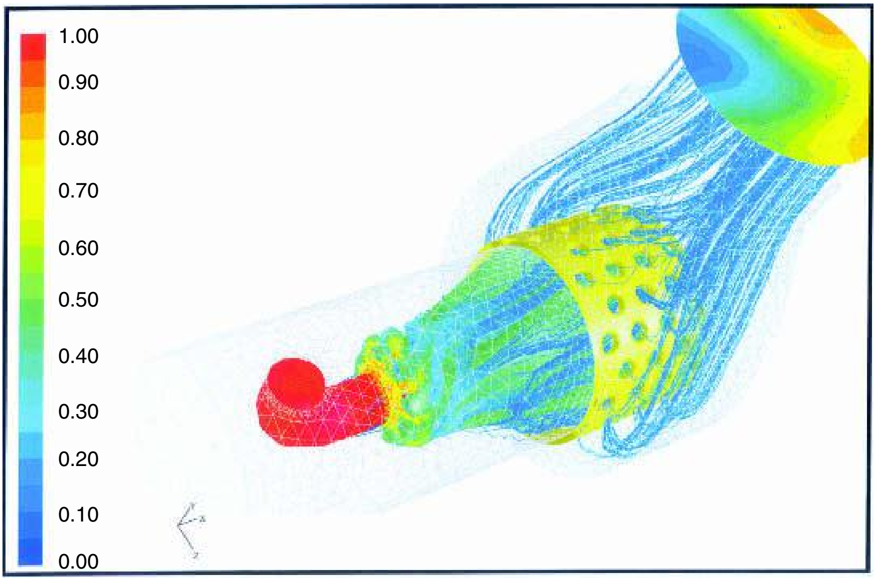


**Figure 20-19** CFD solution for flow in an early tri-phase mixer (GL&V) prior to design modifications. Note the spatial distribution of chemical (chlorine dioxide) in the pipe exiting the mixer.

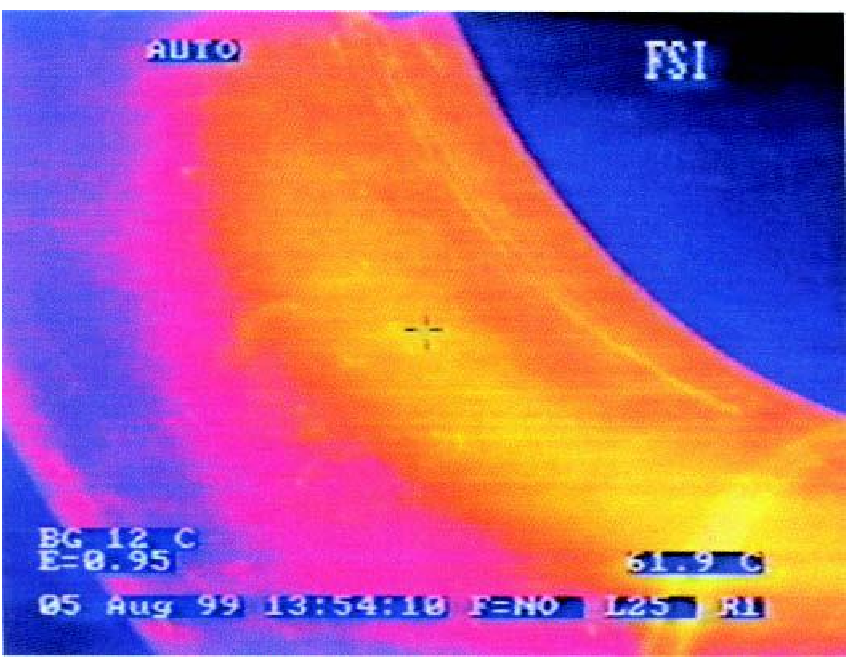


**Figure 20-23** Thermograph of exit piping following a high-shear chlorine dioxide mixer in $D_1$ service. Elbow immediately following mixer discharge. The temperature is 12°C higher along the top of the pipe.

# Practical insights from the leading professionals in the field

While process objectives are critical to the successful manufacturing of a product, if the mixing scale-up fails to produce the required results, the costs of manufacturing can increase significantly. Although there are several industrial operations in which mixing requirements are readily scaled up from established correlations, many operations require a more thorough evaluation. This comprehensive handbook presents the latest methods for recognizing these more complex operations and offers alternative mixing designs for critical applications. The core mixing design topics discussed are:

- Homogeneous blending in tanks and in-line mixers
- Dispersion of gases in liquids with subsequent mass transfer
- Suspension and distribution of solids in liquids
- Liquid-liquid dispersions
- Heat transfer
- Reactions, both homogeneous and heterogeneous

Along with focusing on industrial design and the operation of mixing equipment, the *Handbook of Industrial Mixing* contains summaries of the foundations on which these applications are based. In order to accomplish this, most chapters are written by both an industrialist and an academic. Intended for the practicing engineer who needs to both identify and solve mixing problems, this book also provides concise discussions on theoretical background and uses many illustrative examples when covering applications, and it includes a CD-ROM that contains over fifty video clips and animations of mixing processes. These clips are accompanied by explanatory text.

EDWARD L. PAUL has over thirty-five years' experience in process development with Merck & Co., Inc.

VICTOR A. ATIEMO-OBENG is a scientist in the Engineering Science and Market Development department at The Dow Chemical Company.

SUZANNE M. KRESTA is a professor in the Department of Chemical and Materials Engineering at the University of Alberta.

ISBN 0-471-26919-0

90000

WILEY-INTERSCIENCE
wiley.com

9 780471 269199